AGU PUBLICATIONS

Journal of Advances in Modeling Earth Systems

RESEARCH ARTICLE
10.1002/2014MS000368

Short-term time step convergence in a climate model

Hui Wan[1], Philip J. Rasch[1], Mark A. Taylor[2], and Christiane Jablonowski[3]

[1]Pacific Northwest National Laboratory, Richland, Washington, USA, [2]Sandia National Laboratories, Albuquerque, New Mexico, USA, [3]Department of Atmospheric, Oceanic and Space Sciences, University of Michigan, Ann Arbor, Michigan, USA

Key Points:
- Convergence is slow in CAM5
- Stratiform cloud parameterizations have large errors

Correspondence to:
H. Wan,
Hui.Wan@pnnl.gov

Citation:
Wan, H., P. J. Rasch, M. A. Taylor, and C. Jablonowski (2015), Short-term time step convergence in a climate model, *J. Adv. Model. Earth Syst.*, *7*, 215–225, doi:10.1002/2014MS000368.

Received 23 JUL 2014
Accepted 13 JAN 2015
Accepted article online 20 JAN 2015
Published online 11 FEB 2015

Abstract This paper evaluates the numerical convergence of very short (1 h) simulations carried out with a spectral-element (SE) configuration of the Community Atmosphere Model version 5 (CAM5). While the horizontal grid spacing is fixed at approximately 110 km, the process-coupling time step is varied between 1800 and 1 s to reveal the convergence rate with respect to the temporal resolution. Special attention is paid to the behavior of the parameterized subgrid-scale physics. First, a dynamical core test with reduced dynamics time steps is presented. The results demonstrate that the experimental setup is able to correctly assess the convergence rate of the discrete solutions to the adiabatic equations of atmospheric motion. Second, results from full-physics CAM5 simulations with reduced physics and dynamics time steps are discussed. It is shown that the convergence rate is 0.4—considerably slower than the expected rate of 1.0. Sensitivity experiments indicate that, among the various subgrid-scale physical parameterizations, the stratiform cloud schemes are associated with the largest time-stepping errors, and are the primary cause of slow time step convergence. While the details of our findings are model specific, the general test procedure is applicable to any atmospheric general circulation model. The need for more accurate numerical treatments of physical parameterizations, especially the representation of stratiform clouds, is likely common in many models. The suggested test technique can help quantify the time-stepping errors and identify the related model sensitivities.

1. Introduction

There is an extensive body of literature that documents the horizontal-resolution dependence of atmospheric models and their components. In contrast, much less attention has been paid to the time step sensitivity [e.g., *Teixeira et al.*, 2007], and a major portion of these studies focused on issues associated with convection parameterizations [e.g., *Williamson and Olson*, 2003; *Mishra et al.*, 2008; *Mishra and Sahany*, 2011; *Williamson*, 2013]. Recently, *Wan et al.* [2014] demonstrated substantial sensitivities to time step length in the simulated clouds and precipitation in the Community Atmosphere Model version 5 (CAM5) [*Neale et al.*, 2010]. That study's analysis suggested that the model's time integration was responsible for significant errors at the default temporal resolution. The source of the errors might be the time-stepping methods used inside individual parameterization schemes, and/or the operator-splitting method the model uses to calculate tendencies from separate processes and update the solution. A detailed quantification of the various error sources is a necessary basis for any further efforts that aim at improving the numerical accuracy of the model. This short paper documents one possible approach to such a quantification.

To measure the numerical error, one needs a reference and a metric. Neither is trivial for complex atmospheric models, due to the absence of generic nontrivial analytical solutions to the governing equations. The ultimate "ground truth" for a model simulation is the observed atmospheric motion. However, the discrepancies between simulations and observations are affected by many aspects such as the physical approximations in the equation sets, as well as the initial-data and observation uncertainties. Since our focus here is on the temporal discretization, the error assessments are based on model simulations performed with different time step sizes in the range between 1 and 1800 s. The results obtained with the shortest time step are considered the reference solution. Our assumption is that as the time step size is reduced, the discrete formulation should asymptote to a correct rendering of the intended collection of algebraic and differential equations that are used to express the mathematical model in continuous form. We acknowledge there is no guarantee that the solution obtained with the shortest step size is the closest to the correct solution.

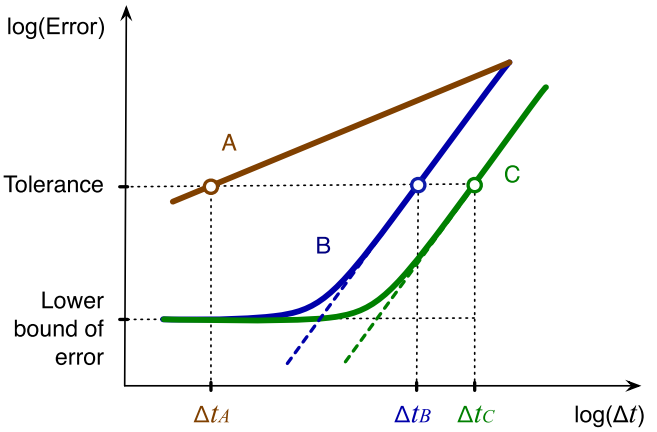

Figure 1. Schematic convergence pathways of three time stepping schemes. Curves B and C denote two schemes that have the same order of accuracy but different magnitudes of error. Line A represents a lower-order scheme. Further details are discussed in section 1.

Nevertheless, it is a good proxy [see e.g., *Teixeira et al*., 2007, 2008], and convergence toward this proxy is a necessary but insufficient condition for the convergence toward the true solution.

If the atmospheric model under consideration is a numerically consistent discretization of a well-posed continuous problem, then the discretization error with respect to the reference solution is expected to level off as the time step is reduced to a sufficiently small value. This is schematically shown in Figure 1 by the blue and green curves which reach a lower bound related to, for example, the accumulation of rounding error discussed by *Rosinski and Williamson* [1997]. In practice, it is often unnecessary to seek a solution to this level of accuracy. The required time step size could easily produce a model that is too expensive to run from a computational viewpoint; hence an error tolerance can be defined through physical reasoning. Once the error of a particular solution falls below that tolerance (see open circles in Figure 1), a "physically reasonable convergence" is achieved, and the quality of the solution becomes practically equivalent to that of the reference solution. The choice of the tolerance depends on the physical quantity in question, and might vary for different scientific investigations. Our study focuses on the numerical convergence. Therefore, the tolerance is established as a concept but is not extensively discussed with respect to the physical flow characteristics.

We chose to characterize the numerical convergence in terms of the root-mean-square error (RMSE) of the 3-dimensional temperature field, and compute the RMSE after a short 1 h integration with the CAM5 model. Temperature is a fundamental and easy-to-use state variable, and is familiar to climate scientists. These features make this variable a desirable choice for model evaluation. Temperature errors are also a characterization of the overall model errors since temperature is coupled to all the other state variables through the model equations. The temperature convergence rate is thereby representative, although the physically acceptable tolerance levels are likely to be different for different variables. We view our discussion of the temperature error in this study as a minimal realization of, or first look at, the comprehensive evaluation of the solution accuracy of all state variables.

All model simulations start from identical initial conditions, and utilize different time step sizes. The 1 h integration time is extremely short and thereby unusual for climate model evaluations, but it has several important advantages. First, by keeping the integration length well within the predictability limit, we can perform deterministic testing without worrying about uncertainties associated with the natural variability or the chaotic nature of the fluid equations [*Lorenz*, 1963]. Second, a 1 h time frame is arguably short enough to minimize the effect of many nonlinear feedback mechanisms, thus facilitating the isolation of errors from individual parameterizations. From a technical viewpoint, a shorter integration time also gives less opportunity for physical or numerical instabilities to grow when physical parameterizations are turned on or off in our sensitivity studies. The initial conditions, which would normally produce smoothly evolving simulations as a result of a balance between forcing terms, can trigger much larger changes when terms in the balance are turned off. If the simulation is short, as it is the case here, the simulations can still be physically reasonable and numerically stable despite the missing forcing mechanisms. Last but not least, the relatively low computational cost enables us to evaluate very short time step lengths (down to 1 s) which would otherwise be prohibitively expensive.

The temperature RMSE allows us to evaluate the order of accuracy (a.k.a. the convergence rate) of CAM5's time-stepping methods. In the spectral-element configuration, the model uses sequential splitting (also known as the Godunov operator splitting or the method of fractional steps) [*Bagrinovskii and Godunov*,

1957; *Yanenko*, 1971] for the coupling between the fluid dynamics solver (the dynamical core) and the parameterized subgrid-scale processes. It means that one model component updates the prognostic variables before handing them to the next component. Such a splitting is formally first-order accurate; therefore, we expect a first-order convergence rate for the full model when assuming that the temporal accuracy inside the individual components are at least first-order.

Our paper addresses the following three CAM5-centered science questions:

1. Does the temperature field converge at the expected first-order rate?

2. What processes are responsible for departures from the expected rate?

3. Is numerical convergence achieved with a 1 s time step?

The remainder of the article is structured as follows. Section 2 briefly introduces the CAM5 model and the experimental design. Section 3 presents a validation of the test procedure via adiabatic dynamical core experiments. The convergence behavior of the full model is discussed in section 4, with the implications discussed in section 5. The summary and conclusions are presented in section 6.

2. Model and Simulation Basics

This study evaluates the convergence properties of CAM version 5.3.07 with its spectral element (SE) dynamical core [*Taylor and Fournier*, 2010; *Dennis et al*., 2012]. The SE dynamics solver employs an explicit, five-stage, third-order-accurate Runge-Kutta (RK) time-stepping scheme, where the extra RK stages are chosen to increase the stability region. Fourth-order hyper-viscosity is applied as a numerical diffusion mechanism. The SE dynamical core offers two options for the vertical discretization. These are an Eulerian finite-difference scheme [*Simmons and Burridge*, 1981] and a floating Lagrangian method [*Lin*, 2004], with the latter being the default choice. The floating Lagrangian approach lets the horizontal flow evolve for brief time before the prognostic variables get remapped back to a vertical reference grid. The vertical reference coordinate is a pressure-based terrain-following hybrid coordinate. The resolved-scale tracer transport employs a three-stage, second-order-accurate, strong-stability-preserving Runge-Kutta (SSP-RK) method with a quasi-monotone limiter [*Guba et al*., 2014].

Parameterized subgrid-scale processes include solar and terrestrial radiation [*Iacono et al*., 2008; *Mlawer et al*., 1997], deep convection [*Zhang and McFarlane*, 1995; *Richter and Rasch*, 2008; *Neale et al*., 2008], shallow convection [*Park and Bretherton*, 2009], moist turbulence [*Bretherton and Park*, 2009], surface exchange processes [*Bryan et al*., 1996; *Lawrence et al*., 2011; *Hunke et al*., 2013], stratiform cloud macrophysics (condensation, evaporation, and cloud fraction) [*Park et al*., 2014], and microphysics [*Morrison and Gettelman*, 2008; *Gettelman et al*., 2008, 2010], as well as aerosol physics and chemistry [*Liu et al*., 2012]. Land surface processes are represented using the Community Land Model version 4 [*Lawrence et al*., 2011].

For stratiform clouds, we also performed sensitivity experiments (see Section 4) using the macrophysics and microphysics parameterizations from the predecessor model CAM4 [*Neale et al*., 2013; *Zhang et al*., 2003; *Rasch and Kristjánsson*, 1998], and the large-scale condensation scheme from the "simple-physics" suite of *Reed and Jablonowski* [2012]. The latter instantaneously converts the moisture in excess of 100% relative humidity to large-scale precipitation without any cloud stages or reevaporation in underlying unsaturated layers.

All simulations presented in this paper used CAM5-SE's "ne30np4" horizontal resolution. This terminology approximately corresponds to a 1° (or 110 km) grid spacing, since each of the six faces of CAM5-SE's cubed-sphere computational mesh is divided into 30×30 elements with 4×4 quadrature points per element. In the vertical direction, the computational domain extends from the Earth's surface to a constant-pressure level at 2 hPa, and is unevenly divided into 30 discrete layers. The layer thicknesses in the hybrid p-σ coordinate change with location and time in either pressure or height; but roughly speaking, the vertical grid spacing is on the order of 60–100 m in the planetary boundary layer, and gradually transitions to about 1 km in the free troposphere. The exact placement of the levels is documented in *Reed and Jablonowski* [2012].

The model's time stepping procedure is complex, and employs different numerical algorithms for the adiabatic fluid dynamics and the subgrid-scale diabatic physics. The time step combinations relevant to this study are listed in Table 1. The time step ratios (rightmost column in Table 1) are optimized to account for the typical time scales or the numerical stability limits of each atmospheric process. In terms of the time

Table 1. Time Step Sizes Used in the Convergence Tests by Various Parts of the CAM5 Model With the SE Dynamical Core[a]

Process or Treatment	Time Step Size (unit: s)							Ratio to Δt
Process coupling with Δt	1	2	8	30	120	450	1800	1
Physics								
Radiation	3600	3600	3600	3600	3600	3600	3600	Varying
Deep convection	1	2	8	30	120	450	1800	1
Shallow convection	1	2	8	30	120	450	1800	1
Stratiform cloud macrophysics	1	2	8	30	120	450	1800	1
Stratiform cloud microphysics[b]	1	2	8	30	120	450	1800	1
SE dynamics								
Vertical remapping[c]	0.5	1	4	15	60	225	900	1/2
Adiabatic fluid dynamics	0.17	0.33	1.33	5	20	75	300	1/6
Resolved-scale tracer transport	0.17	0.33	1.33	5	20	75	300	1/6
Explicit numerical diffusion	0.06	0.11	0.44	1.67	6.67	25	100	1/18

[a]Δt denotes the time interval of numerical coupling between the resolved dynamics and the parameterized physics, and among most (except radiation) parameterizations within the physics package. Further details are provided in section 2.
[b]Including two substeps for the diagnostic rain and snow equations.
[c]Only relevant to the Lagrangian vertical discretization.

integration procedure of the whole model, the frequency at which the resolved dynamics and various parameterized physical processes are coupled together plays the central role, as further explained below. We refer to this step size as the "process-coupling" time step, and denote it by Δt hereafter.

Although individual parameterizations may employ substepping, and often use different numerical algorithms (e.g., the Euler forward scheme, predictor-corrector methods, or implicit algorithms), they each invariably update the model state variables at an interval Δt before giving the control to the next parameterization. Short-wave and long-wave radiative heating rates are typically computed at longer (hourly) time intervals to reduce their computational cost. Those tendencies are then kept constant, and used for the state variable updates at the same interval Δt as other parameterizations. In the dynamical core, different time step sizes are employed for the tracer transport, vertical remapping, and the adiabatic dynamics. These shorter time steps are implemented as substeps with respect to Δt. During an interval Δt, the SE dynamical core operates on its own without exchanging information with the parameterized physics. Furthermore, when CAM5 communicates with CLM4 (or the ocean and sea-ice models in a fully coupled mode, which we do not use in this study), the Δt defined above is referred to as the atmosphere model time step, and is also used by the coupler to determine when exchanges of surface fluxes should occur.

The default process-coupling time step for the 1°, 30 layer model configuration is $\Delta t = 1800$ s with radiative tendencies calculated every hour. Within the dynamical core, vertical remapping is performed every 900 s. Tracer advection and adiabatic dynamics are subcycled using a step size of 300 s. The explicit numerical diffusion, employed in the form of hyperviscosity, uses time steps of 100 s (Table 1). In our convergence tests, we decreased the process-coupling time step Δt from 1800 to 450, 120, 30, 8, 2 and 1 s, and proportionally reduced the step sizes in the dynamics components (Table 1). In case the physical parameterizations needed subcycling, the either fixed or interactively determined number of iterations were kept unchanged. Radiative heating rates were calculated hourly and applied at every coupling time step.

The simulations with the shortest time step ($\Delta t = 1$ s) are considered reference solutions. Departures from the reference solution are expressed as a temperature RMSE following *Rosinski and Williamson* [1997]:

$$\mathrm{RMSE}(T) = \left\{ \frac{\sum_i \sum_k w_i [\Delta T(i,k)]^2 \Delta \bar{p}(i,k)}{\sum_i \sum_k w_i \Delta \bar{p}(i,k)} \right\}^{1/2}, \tag{1}$$

$$\Delta T(i,k) = T(i,k) - T_r(i,k), \tag{2}$$

$$\Delta \bar{p}(i,k) = [\Delta p(i,k) + \Delta p_r(i,k)]/2. \tag{3}$$

Here $\Delta p(i,k)$ denotes the pressure-layer thickness on vertical level k at grid cell i. w_i is the area of cell i. Subscript r indicates the reference solution. The sums in equation (1) are taken over all grid cells of the horizontal mesh and all layers of the vertical grid.

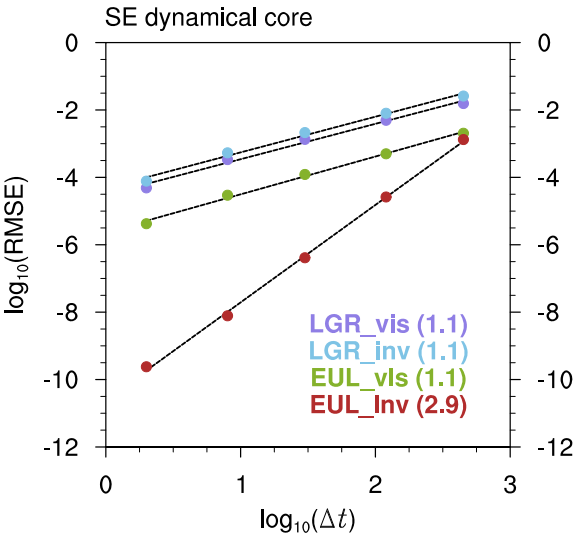

Figure 2. Dependence of the temperature RMSE (in K, cf. equation (1)) on the physics-dynamics coupling time step Δt (in s) in 1 h dry adabatic simulations that were conducted with the SE dynamical core using real-world land-sea mask and topography. The Lagrangian and Eulerian vertical discretization schemes are referred to as "LGN" and "EUL", respectively. Simulations with the standard hyperviscosity are denoted by "vis", and those without viscosity by "inv". Colored dots show the temperature RMSE calculated over all grid cells of the horizontal mesh and all levels of the vertical grid. Dashed lines are linear fits between $\log_{10}$(RMSE) and $\log_{10}(\Delta t)$. The convergence rates are given in parenthesis. We note that the results in this figure were obtained without physics parameterization, but the errors are plotted against the physics-dynamics coupling time step Δt for consistency with other figures. The entire 3-D domain was included in the calculation of the RMSE.

3. Tests With the Dynamical Core

As a proof of concept, we first present results from dry, adiabatic simulations with the SE dynamical core. All subgrid-scale physical parameterizations were switched off, and the initial concentrations of water species were set to zero. However, all other initial conditions were taken from a spun-up CAM5-SE climate simulation and utilized real-world topography and land-sea masks. We deliberately chose to perform such "realistic" adiabatic simulations instead of the idealized tests recommended by, e.g., the Dynamical Core Intercomparison Project (DCMIP, https://www.earthsystemcog.org/projects/dcmip-2012/) or by *Jablonowski and Williamson* [2006], to facilitate the comparison with the full-physics results in section 4.

Four configurations of the SE dynamical core were tested which used different combinations of the vertical discretization methods (floating Lagrangian ("LGR") versus Eulerian ("EUL")) and the hyperviscosity setting (inviscid without diffusion ("inv") versus standard diffusion ("vis")). The convergence properties of these combinations are shown in Figure 2. The figure displays the temperature RMSE versus the process-coupling time step Δt in a double-logarithmic diagram. Recall that the dynamics time steps are shorter than Δt as shown in Table 1, but Δt is plotted here for consistency with other figures. The dashed lines are linear fits between the actual data points which are denoted by colored dots. The convergence rates are noted in parentheses.

The vertically Eulerian, inviscid simulations ("EUL_inv") are expected to show third-order convergence which is inherent of CAM5-SE's RK method. When hyperviscosity is applied ("EUL_vis"), the solutions are expected to converge at a first-order rate when the horizontal spacing Δx is fixed. This is due to the Euler forward scheme that the explicitly-added diffusion equation utilizes. We note that the solutions would converge at a third-order rate if Δx and Δt were reduced together, since in practice the hyperviscosity coefficient is set proportionally to $\Delta x^{3.2}$. The Lagrangian vertical discretization ("LGR") is also expected to reduce the convergence rate to first-order, due to the utilization of monotonic limiter and the fact that the vertical remapping uses sequential operator splitting. The RMSE characteristics in Figure 2 indeed reveal the expected behavior.

To evaluate the uncertainties in the estimated convergence rates, we repeated the dynamical core tests with different initial conditions (not shown). We found that the absolute magnitudes of the temperature error may differ from case to case, but the estimated convergence rates are rather insensitive to the starting state of the simulations. In addition, the qualitative conclusions regarding the relative accuracy stay unchanged. Namely, the vertically Lagrangian scheme without viscosity ("LGR_inv") is associated with the largest temperature error, while the vertically Eulerian, inviscid version ("EUL_inv") leads to the smallest RMSE among the four configurations. These results suggest that the test procedure based on the temperature RMSE of 1 h simulations is capable of providing a reliable characterization of the time step convergence rate in the global model.

4. Results With Diabatic Physics

The added complexity of parameterized subgrid-scale physics may lead to larger uncertainties in the estimated convergence rate. Therefore, ensemble simulations with six members were performed using

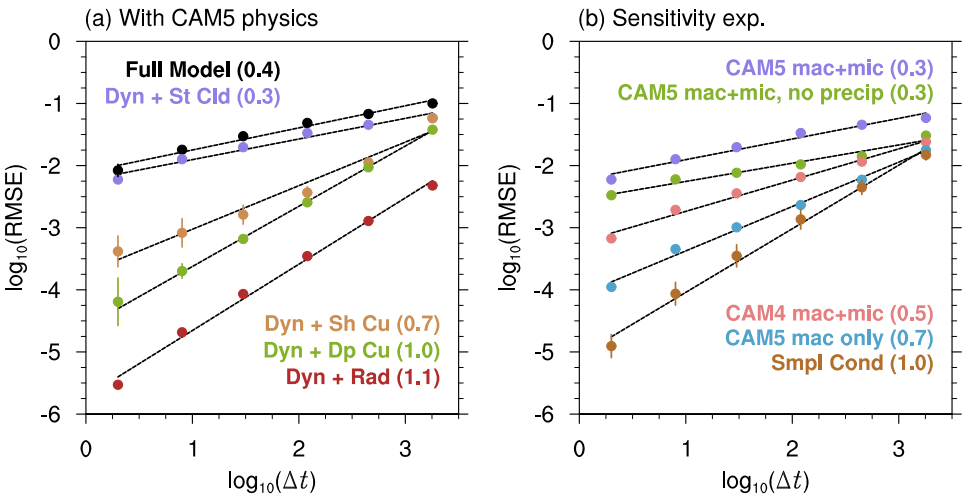

Figure 3. Similar to Figure 2 but for moist simulations conducted with subgrid-scale physics parameterization. Dots: average $\log_{10}$(RMSE) of six ensemble simulations. Vertical bars: ensemble standard deviation of $\log_{10}$(RMSE). "Full Model": standard CAM5-SE configuration with real-world land-sea mask and topography. All other simulations: SE dynamical core (Dyn) plus one parameterization in an aqua-planet setup. "St Cld": stratiform cloud macrophysics and microphysics; "Sh Cu" and "Dp Cu": shallow and deep cumulus convection; "Rad": radiation. "CAM5 mac+mic" in Figure 3b and "Dyn + St Cld" in Figure 3a refer to the same group of simulations. "CAM5 mac+mic, no precip": similar to "CAM5 mac+mic", but without the formation and sedimentation of rain and snow. "CAM5 mac only": CAM5 cloud macrophysics scheme was switched on but the stratiform cloud microphysics was turned off. "CAM4 mac+mic": stratiform cloud parameterizations from CAM4. "Smpl Cond": simplified representation of large-scale condensation following *Reed and Jablonowski* [2012]. The entire 3-D domain was included in the calculation of the RMSE.

independent atmospheric states for the initial conditions. The ensemble-mean temperature error and the standard deviation of the six members are shown in Figure 3 with thick dots and vertical bars, respectively.

The first simulation set in this section includes a land-sea mask and realistic topography, with differing surface fluxes over land and ocean for momentum, heat, moisture, and trace constituents. These are referred to as the "full model" simulations in the text below and in Figure 3. Somewhat unexpectedly, solutions from the full model converge rather slowly at a rate of 0.4 instead of 1.0. Compared to the results in the previous section, the RMSE temperature errors are much higher for any choice of Δt. For example, they are 0.1 K with the default 1800 s coupling time step and 0.01 K with a 2 s time step. Figure 4 (left) shows the corresponding histograms of the temperature error (assessed in the global domain). The histograms indicate that, despite the rather short integration period, local errors on the order of 1 K can be found at a nonnegligible

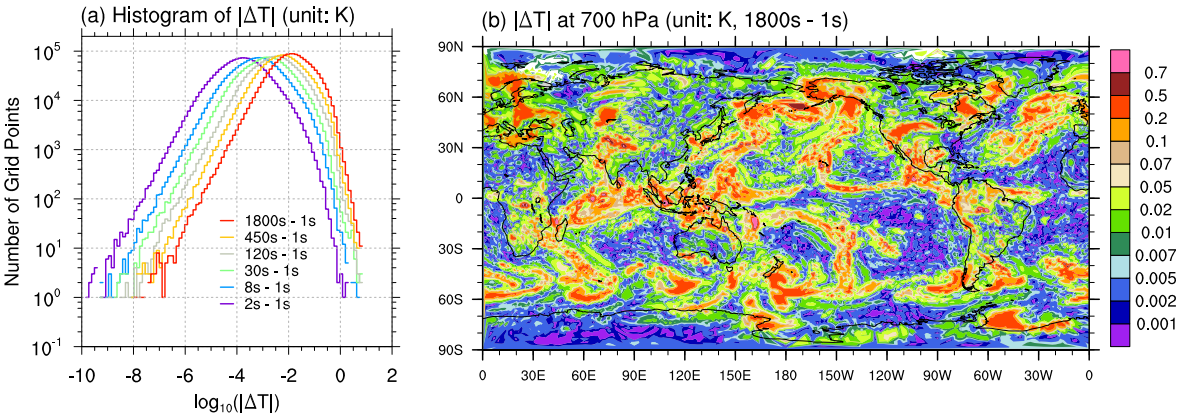

Figure 4. Analysis of the "Full Model" CAM5 simulations in Figure 3a: (a) Histogram of the absolute temperature difference (in K) between the reference simulation and the simulations with longer time steps. The sampling region is the entire 3-D domain. (b) Geographical distribution of the 700 hP absolute temperature difference (in K) between the $\Delta t = 1800$ s and 1 s time step simulations.

number of grid points. Smaller errors (i.e., left halves of the histograms) converge at a first-order rate, while the largest errors are not reduced as fast. This suggests that the slow convergence might be attributable to certain climate regimes and/or physical processes. Figure 4 (right) shows the geographical distribution of the 700 hPa temperature error. The characteristic patterns give a clear hint that the largest errors occur primarily in regions with clouds and/or precipitation.

To identify which processes or interactions were responsible for the slow convergence, we conducted a series of sensitivity simulations. First, we simplified the problem and switched from the real world to an aqua-planet configuration following the experimental design of *Neale and Hoskins* [2000]. These aqua-planet convergence results were very similar to those from the real-world full-physics simulations, and are therefore not shown. This indicates that the topography and the land-surface processes are not the cause of the convergence problem.

In order to isolate causes and effects, we then tested the physical parameterizations in isolation by using the dynamical core plus one parameterization at a time. This set of simulations were also conducted in the aqua-planet mode. Figure 3a shows selected examples where we paired the dynamical core ("Dyn") with the stratiform cloud macrophysics and microphysics ("St Cld"), the shallow cumulus convection ("Sh Cu"), the deep cumulus convection ("Dp Cu"), and radiation ("Rad"). The convergence rates are listed in parentheses. Clearly the diagram indicates that the time-stepping errors differ substantially in individual parameterizations.

The radiative transfer and cooling/heating calculations introduce very little error in the absence of clouds (Figure 3a, dark red dots). The dynamics-only aqua-planet simulations, although not shown in the figure, are virtually indistinguishable from the "Dyn + Rad" simulations.

The first-order convergence of the "Dyn + Dp Cu" simulations (Figure 3a, green dots) might seem surprisingly "fast" at first, but displays the expected behavior. The deep convection parameterization in CAM5 is a mass-flux scheme [*Zhang and McFarlane*, 1995]. The strength of the convective activities, and hence their feedback to the large-scale environment, is ultimately determined using the assumption that the convective available potential energy (CAPE) is restored to an equilibrium state on a certain time scale. Both the equilibrium CAPE and the convective adjustment time scale are empirical constants in CAM5. Such a relaxation is expected to help ensure first-order convergence. By contrast, a moist adiabatic adjustment scheme explicitly resets the state of the model column to a moist adiabatic profile within one time step. In this case, the subgrid-scale processes that lead to the "desired" neutral state cannot (and are not meant to) be temporally resolved. The interplay between the related buoyancy change, vertical motion, and the phase change of water species might be highly nonlinear and numerically challenging. It will be interesting to test the convergence property of such an adjustment scheme as well as other convection parameterizations that use closure assumptions different from the one in the *Zhang and McFarlane* [1995] parameterization.

Another interesting result revealed by Figure 3a is that the relationship between log(RMSE) and log(Δt) is nonlinear in the "Dyn + Sh Cu" simulations (Figure 3a, brown dots). We have not yet conducted any further analyses of the shallow convection parameterization, thus the causes for this behavior are unclear. Nevertheless, the temperature error does decrease with reduced time step size. Furthermore, the RMSE associated with shallow convection is about one order of magnitude smaller than that associated with the stratiform cloud parameterizations.

It is evident that the full-model real-world simulations (Figure 3a, black dots) and the "Dyn + St Cld" aqua-planet simulations (Figure 3a, purple dots) have similar temperature RMSE. This suggests that the stratiform cloud parameterizations are a major source of numerical error, which might be an expected result when considering the large number of highly nonlinear processes in this part of the model. In addition, a large number of physical approximations are required to make the representation of the small-scale processes computationally affordable in a global climate model. The complex connections between aerosols and clouds [*Liu et al*., 2012], the treatment of ice supersaturation and nucleation [*Gettelman et al*., 2010], and the variety of precipitation-related processes [*Morrison and Gettelman*, 2008; *Gettelman et al*., 2008] pose big challenges to the design of time-stepping methods. Additional simulations using the dynamical core plus only the macrophysics ("CAM5 mac only" in Figure 3b) show substantially smaller errors, confirming that the main difficulty lies indeed in the microphysics package.

Over the past few years, efforts have been underway to replace the diagnostic rain and snow representation in the cloud microphysics parameterization with a prognostic treatment [*Gettelman and Morrison*, 2014; *Gettelman et al*., 2014a]. The new formulation provides an improved representation of the relative balance between different rain formation mechanisms [*Gettelman and Morrison*, 2014; *Gettelman et al*., 2013, 2014a, 2014b]. Therefore, it is a logical next step to ask whether these changes also alleviate the numerical convergence problem. Once the new prognostic treatment becomes available in CAM, the updated microphysics package will be tested. Alternatively, we performed a set of sensitivity simulations with the current microphysics parameterization but without the rain and snow formation or sedimentation. These are the "CAM5 mac+mic, no precip" simulations in Figure 3b. In such a model configuration, the liquid-phase and ice-phase cloud condensates can be generated by large-scale condensation and vapor deposition (including the Bergeron process) in terms of mass concentration, and by droplet activation and ice nucleation in terms of number concentration. The removal mechanisms include droplet evaporation, ice sublimation, and condensate sedimentation. The temperature errors in this set of simulations are shown by the green dots in Figure 3b. The convergence rate is similar to that of the simulations with diagnostic precipitation, while the magnitude of the temperature RMSE is about a factor-of-two smaller. In other words, the diagnostic precipitation equations seem to contribute to the total error, but do not determine the rate of convergence. We speculate that the time step sensitivity of the ice cloud microphysics in the current model needs to be carefully examined. Whether the new microphysics parameterization will bring substantial improvement remains to be answered in the future.

For further comparison, we also tested the stratiform cloud parameterization of the CAM4 model coupled with the SE dynamical core. Under this configuration, we got smaller temperature errors compared to CAM5, but still a rather slow convergence rate (0.5, Figure 3b, pink dots). The CAM4 and CAM5 microphysics schemes have very little in common in terms of the continuous formulation and the numerical treatments. It is curious that they both appear to have convergence issues. Future investigations are planned to obtain an in-depth understanding of the behavior of these schemes. As an aside, the simple large-scale condensation scheme of *Reed and Jablonowski* [2012] converges at first-order ("Smpl Cond"). This may seem trivial, but provides useful information. In the absence of a subgrid-scale cloudiness scheme which might complicate the situation, the assumption that the condensation of water vapor is fast and always occurs within one time step Δt does not degrade the numerical convergence.

5. Implications

The results from our convergence test have far-reaching impact. First, the convergence rate discussed in this paper is not just a mathematical concept of mere academic interest. It is of clear practical relevance because both plots of Figure 3 indicate that, at least for the parameterizations tested in this study, the convergence rate is inversely correlated with absolute error. In other words, a parameterization that converges slower also has larger time stepping error. There is no obvious theoretical reason for this behavior. In principle, it may be possible to construct implicit or semiimplicit time stepping schemes for certain parameterizations that appear to be low-order but highly accurate, giving a temperature RMSE smaller than, say, 10^{-3} K with a 1800 s time step. In such a case, the low-order convergence would not be of concern. But this type of behavior is not seen in Figure 3, and will be a target for future work.

Second, the numerical errors shown in Figures 2 and 3 also reveal the parameterization schemes' time step sensitivity. In the tested step-size range, the lower-order parameterizations have stronger time step sensitivities than the higher-order schemes. This can be seen more clearly from Figure 5 which shows the same convergence diagrams as in Figure 3 but with a linear scale for the *y* axes.

Over the past decade, global climate models have tended to incorporate new and more complex cloud parameterizations in order to integrate more physically based representations of the atmospheric water cycle and the aerosol-climate interactions [e.g., *Lohmann et al*., 2007; *Posselt and Lohmann*, 2008; *Lohmann and Hoose*, 2009; *Wilson et al*., 2008a, 2008b; *Morrison and Gettelman*, 2008; *Gettelman et al*., 2008, 2010; *Salzmann et al*., 2010]. Some recent studies have found that algorithmic details in the cloud microphysics parameterizations can significantly affect the simulated cloud properties, precipitation rate, and aerosol

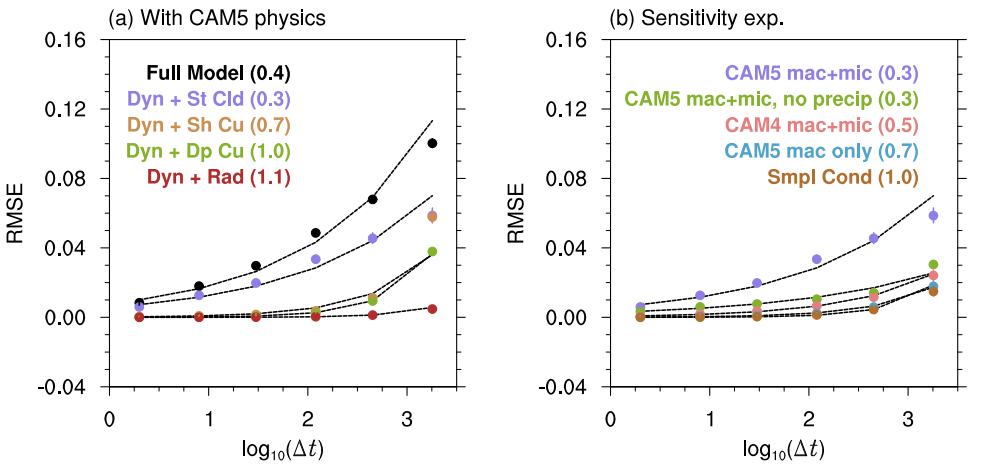

Figure 5. As in Figure 3 but using linear scales for the *y* axes.

indirect effects [e.g., *Morrison and Gettelman*, 2008; *Posselt and Lohmann*, 2008, 2009; *Salzmann et al.*, 2010; *Gettelman and Morrison*, 2014; *Gettelman et al.*, 2014a]. Our results obtained from the time step convergence test indicate that the impact of the numerical treatment in the stratiform cloud parameterizations is not limited to clouds and precipitation. Rather, it quickly translates into numerical errors and time step sensitivities in the temperature field which is of fundamental importance for climate and weather modelers. Although our short-term time step convergence test has only been applied to CAM5, the conclusion that stratiform cloud parameterizations are a major source of time stepping error is probably valid in many other models. Unfortunately, there is a lack of systematic investigations in the climate modeling community concerning the efficient and accurate numerical treatments of cloud microphysics in global models. We believe that more attention needs to be paid to this research topic, and in a broader sense, to the numerical issues in physical parameterizations in general.

6. Conclusions

We have demonstrated that a time step convergence test based on the temperature RMSE of 1 h simulations provides useful information about the time stepping errors in various components of the climate model CAM5. Even for such a complex model, the convergence rate is still a relevant metric. Our results indicate that parameterization schemes with slow convergence rates are associated with larger errors and stronger time step sensitivity.

With a 1 s time step length, we did not obtain a solution that had converged in the numerical sense to round-off level. The temperature error in CAM5 converged at a rate of 0.4, substantially slower than the expected first-order convergence. Sensitivity experiments were performed to test individual parameterizations in isolation. These showed that the slow convergence of the full model is primarily attributable to the stratiform cloud parameterizations, in particular the cloud microphysics. Processes that produce the slowest convergence rates also produce the largest errors, providing a "flag" for model components that do not accurately represent the intended physical balance of processes, and thus require more attention.

This paper demonstrates the problem but does not explain the root cause of it. We will further explore the issue. Once understood, our intention is to suggest alternate discrete formulations that provide better accuracy at a reasonable computational cost. In the long run, it may be useful to include such convergence tests in the standard test suite of CAM, and conduct them after each major update of the model components. Since the convergence test is straightforward to implement and computationally inexpensive, it should be applicable to any other atmospheric general circulation model. A continuous monitoring of the time stepping error will help to keep the numerical artifacts under control, and assure that a discrete model indeed reflects the intended representation of the physical processes.

Acknowledgments

The authors thank Balwinder Singh, Heng Xiao, Kai Zhang, Jin-ho Yoon, Minghuai Wang, and Po-Lun Ma for valuable discussions. The two anonymous reviewers are thanked for their comments and suggestions. H. Wan acknowledges support from the Linus Pauling Distinguished Postdoctoral Fellowship of the Pacific Northwest National Laboratory (PNNL) and the PNNL Laboratory Directed Research and Development Program. PNNL is operated by Battelle Memorial Institute for the U.S. Department of Energy (DOE) under contract DE-AC05-76RL01830. P. J. Rasch was supported by the DOE Office of Science as part of the Scientific Discovery through Advanced Computing (SciDAC) Program. M. A. Taylor was supported by the DOE Office of Biological and Environmental Research, work package 11-014996, "Climate Science for a Sustainable Energy Future". C. Jablonowski was supported by the DOE Office of Science SciDAC award DE-SC0006684. This research used resources of the Oak Ridge Leadership Computing Facility at the Oak Ridge National Laboratory, which is supported by the Office of Science of DOE under contract DE-AC05-00OR22725. The allocation was awarded under DOE's ASCR Leadership Computing Challenge (ALCC) program in support of the Aerosol Clouds and Precipitation Scientific Focus Area of the DOE Earth System Modeling Program. Data discussed in the paper are available upon request from the corresponding author.

References

Bagrinovskii, K. A., and S. K. Godunov (1957), Difference schemes for multidimensional problems, *Dokl. Akad. Nauk SSSR*, *115*, 431–433.

Bretherton, C. S., and S. Park (2009), A new moist turbulence parameterization in the Community Atmosphere Model, *J. Clim.*, *22*, 3422–3448, doi:10.1175/2008JCLI2556.1.

Bryan, F. O., B. G. Kauffman, W. G. Large, and P. R. Gent (1996), The NCAR CSM flux coupler, *NCAR Tech. Note NCAR/TN-424+STR*, *Natl. Cent. for Atmos. Res.*, Boulder, Colo., doi:10.5065/D6QV3JG3.

Dennis, J. M., J. Edwards, K. J. Evans, O. Guba, P. H. Lauritzen, A. A. Mirin, A. St-Cyr, M. A. Taylor, and P. H. Worley (2012), CAM-SE: A scalable spectral element dynamical core for the Community Atmosphere Model, *Int. J. High Perform. Comput. Appl.*, *26*, 74–89, doi:10.1177/1094342011428142.

Gettelman, A., and H. Morrison (2014), Advanced two-moment microphysics for global models. Part I: Off-line tests and comparisons with other schemes, *J. Clim.*, doi:10.1175/JCLI-D-14-00102.1.

Gettelman, A., H. Morrison, and S. J. Ghan (2008), A new two-moment bulk stratiform cloud microphysics scheme in the Community Atmosphere Model, version 3 (CAM3). Part II: Single-column and global results, *J. Clim.*, *21*, 3660–3679, doi:10.1175/2008JCLI2116.1.

Gettelman, A., X. Liu, S. J. Ghan, H. Morrison, S. Park, A. J. Conley, S. A. Klein, J. Boyle, D. L. Mitchell, and J.-F. L. Li (2010), Global simulations of ice nucleation and ice supersaturation with an improved cloud scheme in the Community Atmosphere Model, *J. Geophys. Res.*, *115*, D18216, doi:10.1029/2009JD013797.

Gettelman, A., H. Morrison, C. R. Terai, and R. Wood (2013), Microphysical process rates and global aerosol-cloud interactions, *Atmos. Chem. Phys.*, *13*, 9855–9867, doi:10.5194/acp-13-9855-2013.

Gettelman, A., H. Morrison, S. Santos, P. Bogenschutz, and P. H. Caldwell (2014a), Advanced two-moment microphysics for global models. Part II: Global model solutions and aerosol-cloud interactinos, *J. Clim.*, doi:10.1175/JCLI-D-14-00103.1.

Gettelman, A., H. Morrison, C. R. Terai, and R. Wood (2014b), Corrigendum to "Microphysical process rates and global aerosol-cloud interactions" published in Atmos. Chem. Phys., 13, 9855–9867, 2013, *Atmos. Chem. Phys.*, *14*, 9099–9103, doi:10.5194/acp-14-9099-2014.

Guba, O., M. A. Taylor, and A. St.-Cyr (2014), Optimization-based limiters for the spectral element method, *J. Comput. Phys.*, *267*, 176–195, doi:10.1016/j.jcp.2014.02.029.

Hunke, E. C., W. H. Lipscomb, A. K. Turner, N. Jeffery, and S. Elliott (2013), CICE: The Los Alamos sea ice model documentation and software user's manual version 5.0, *Los Alamos National Laboratory Tech. Rep. LA-CC-06-012*, Los Alamos Natl. Lab., Los Alamos, N. M.

Iacono, M., J. Delamere, E. Mlawer, M. Shephard, S. Clough, and W. Collins (2008), Radiative forcing by long-lived greenhouse gases: Calculations with the AER radiative transfer models, *J. Geophys. Res.*, *113*, D13103, doi:10.1029/2008JD009944.

Jablonowski, C., and D. L. Williamson (2006), A baroclinic instabilitiy test case for atmospheric model dynamical cores, *Q. J. R. Meteorol. Soc.*, *132*, 2943–2975, doi:10.1256/qj.06.12.

Lawrence, D. M., et al. (2011), Parameterization improvements and functional and structural advances in Version 4 of the Community Land Model, *J. Adv. Model. Earth Syst.*, *3*, M03001, doi:10.1029/2011MS000045.

Lin, S.-J. (2004), A "vertically Lagrangian" finite-volume dynamical core for global models, *Mon. Weather Rev.*, *132*, 2293–2307, doi:10.1175/1520-0493(2004)132<2293:AVLFDC>2.0.CO;2.

Liu, X., et al. (2012), Toward a minimal representation of aerosols in climate models: Description and evaluation in the Community Atmosphere Model CAM5, *Geosci. Model Dev.*, *5*(3), 709–739, doi:10.5194/gmd-5-709-2012.

Lohmann, U., and C. Hoose (2009), Sensitivity studies of different aerosol indirect effects in mixed-phase clouds, *Atmos. Chem. Phys.*, *9*, 8917–8934, doi:10.5194/acp-9-8917-2009.

Lohmann, U., P. Stier, C. Hoose, S. Ferrachat, S. Kloster, E. Roeckner, and J. Zhang (2007), Cloud microphysics and aerosol indirect effects in the global climate model ECHAM5-HAM, *Atmos. Chem. Phys.*, *7*, 3425–3446, doi:10.5194/acp-7-3425-2007.

Lorenz, E. N. (1963), Deterministic nonperiodic flow, *J. Atmos. Sci.*, *20*, 130–141, doi:10.1175/1520-0469(1963)020<0130:DNF>2.0.CO;2.

Mishra, S. K., and S. Sahany (2011), Effects of time step size on the simulation of tropical climate in NCAR-CAM3, *Clim. Dyn.*, *37*, 689–704, doi:10.1007/s00382-011-0994-4.

Mishra, S. K., J. Srinivasan, and R. S. Nanjundiah (2008), The impact of the time step on the intensity of ITCZ in an aquaplanet GCM, *Mon. Weather Rev.*, *136*, 4077–4091, doi:10.1175/2008MWR2478.1.

Mlawer, E. J., S. J. Taubman, P. D. Brown, M. J. Iacono, and S. A. Clough (1997), Radiative transfer for inhomogeneous atmospheres: RRTM, a validated correlated-k model for the longwave., *J. Geophys. Res.*, *102*, 16,663–16,682, doi:10.1029/97JD00237.

Morrison, H., and A. Gettelman (2008), A new two-moment bulk stratiform cloud microphysics scheme in the NCAR Community Atmosphere model (CAM3), Part I: Description and numerical tests, *J. Clim.*, *21*, 3642–3659, doi:10.1175/2008JCLI2105.1.

Neale, R. B., and B. J. Hoskins (2000), A standard test for AGCMs including their physical parameterizations: I: The proposal, *Atmos. Sci. Lett.*, *1*, 101–107, doi:10.1006/asle.2000.0022.

Neale, R. B., J. H. Richter, and M. Jochum (2008), The impact of convection on ENSO: From a delayed oscillator to a series of events, *J. Clim.*, *21*, 5904–5924, doi:10.1175/2008JCLI2244.1.

Neale, R. B., et al. (2010), Description of the NCAR Community Atmosphere Model (CAM5.0), *NCAR Tech. Note NCAR/TN-486+STR*, Natl. Cent. for Atmos. Res., Boulder, Colo.

Neale, R. B., J. Richter, S. Park, P. H. Lauritzen, S. J. Vavrus, P. J. Rasch, and M. Zhang (2013), The mean climate of the Community Atmosphere Model (CAM4) in forced SST and fully coupled experiments, *J. Clim.*, *26*, 5150–5168, doi:10.1175/JCLI-D-12-00236.1.

Park, S., and C. S. Bretherton (2009), The University of Washington shallow convection and moist turbulence schemes and their impact on climate simulations with the Community Atmosphere Model, *J. Clim.*, *22*, 3449–3469, doi:10.1175/2008JCLI2557.1.

Park, S., C. S. Bretherton, and P. J. Rasch (2014), Integrating cloud processes in the Community Atmosphere Model, version 5., *J. Clim.*, *27*, 6821–6855, doi:10.1175/JCLI-D-14-00087.1.

Posselt, R., and U. Lohmann (2008), Introduction of prognostic rain in ECHAM5: Design and single column model simulations, *Atmos. Chem. Phys.*, *8*, 2949–2963, doi:10.5194/acp-8-2949-2008.

Posselt, R., and U. Lohmann (2009), Sensitivity of the total anthropogenic aerosol effect to the treatment of rain in a global climate model, *Geophys. Res. Lett.*, *36*, L02805, doi:10.1029/2008GL035796.

Rasch, P. J., and J. E. Kristjánsson (1998), A comparison of the CCM3 model climate using diagnosed and predicted condensate parameterizations, *J. Clim.*, *11*, 1587–1614, doi:10.1175/1520-0442(1998)011<1587:ACOTCM>2.0.CO;2.

Reed, K. A., and C. Jablonowski (2012), Idealized tropical cyclone simulations of intermediate complexity: A test case for AGCMs, *J. Adv. Model. Earth Syst.*, *4*, M04001, doi:10.1029/2011MS000099.

Richter, J. H., and P. J. Rasch (2008), Effects of convective momentum transport on the atmospheric circulation in the Community Atmosphere Model, version 3, *J. Clim.*, *21*, 1487–1499, doi:10.1175/2007JCLI1789.1.

Rosinski, J. M., and D. L. Williamson (1997), The accumulation of rounding errors and port validation for global atmospheric models, *SIAM J. Sci. Comput.*, *18*, 552–564, doi:10.1137/S1064827594275534.

Salzmann, M., Y. Ming, J.-C. Golaz, P. A. Ginoux, H. Morrison, A. Gettelman, M. Krämer, and L. J. Donner (2010), Two-moment bulk stratiform cloud microphysics in the GFDL AM3 GCM: Description, evaluation, and sensitivity tests, *Atmos. Chem. Phys.*, *10*, 8037–8064, doi:10.5194/acp-10-8037-2010.

Simmons, A. J., and D. M. Burridge (1981), An energy and angular-momentum conserving vertical finite difference scheme and hybrid vertical coordinates, *Mon. Weather Rev.*, *109*, 758–766, doi:10.1175/1520-0493(1981)109<0758:AEAAMC>2.0.CO;2.

Taylor, M. A., and A. Fournier (2010), A compatible and conservative spectral element method on unstructured grids, *J. Comput. Phys.*, *229*, 5879–5895, doi:10.1016/j.jcp.2010.04.008.

Teixeira, J., C. A. Reynolds, and K. Judd (2007), Time step sensitivity of nonlinear atmospheric models: Numerical convergence, truncation error growth, and ensemble design, *J. Atmos. Sci.*, *64*, 175–189, doi:10.1175/JAS3824.1.

Teixeira, J., C. A. Reynolds, and K. Judd (2008), Reply, *J. Atmos. Sci.*, *65*, 683–684, doi:10.1175/2007JAS2523.1.

Wan, H., P. J. Rasch, K. Zhang, Y. Qian, H. Yan, and C. Zhao (2014), Short ensembles: An efficient method for discerning climate-relevant sensitivities in atmospheric general circulation models, *Geosci. Model Dev.*, *7*, 1961–1977, doi:10.5194/gmd-7-1961-2014.

Williamson, D. L. (2013), The effect of time steps and time-scales on parametrization suites, *Q. J. R. Meteorol. Soc.*, *139*, 548–560, doi:10.1002/qj.1992.

Williamson, D. L., and J. G. Olson (2003), Dependence of aqua-planet simulations on time step, *Q. J. R. Meteorol. Soc.*, *129*, 2049–2064, doi:10.1256/qj.02.62.

Wilson, D. R., A. C. Bushell, A. M. Kerr-Munslow, J. D. Price, and C. J. Morcrette (2008a), PC2: A prognostic cloud fraction and condensation scheme. I: Scheme description, *Q. J. R. Meteorol. Soc.*, *134*, 2093–2107, doi:10.1002/qj.333.

Wilson, D. R., A. C. Bushell, A. M. Kerr-Munslow, J. D. Price, C. J. Morcrette, and A. Bodas-Salcedo (2008b), PC2: A prognostic cloud fraction and condensation scheme. II: Climate model simulations, *Q. J. R. Meteorol. Soc.*, *134*, 2109–2125, doi:10.1002/qj.332.

Yanenko, N. N. (1971), *The Method of Fractional Steps: The Solution of Problems of Mathematical Physics in Several Variables*, 160 pp., Springer-Verlag, Berlin Heidelberg. doi:10.1007/978-3-642-65108-3.

Zhang, G. J., and N. A. McFarlane (1995), Sensitivity of climate simulations to the parameterization of cumulus convection in the Canadian Climate Centre general circulation model, *Atmos. Ocean*, *33*, 407–446, doi:10.1080/07055900.1995.9649539.

Zhang, M., W. Lin, C. S. Bretherton, J. J. Hack, and P. J. Rasch (2003), A modified formulation of fractional stratiform condensation rate in the NCAR Community Atmospheric Model (CAM2), *J. Geophys. Res.*, *108*(D1), 4035, doi:10.1029/2002JD002523.